Level Scheme and Configuration Mixing in Sc^{44}†

J. J. SCHWARTZ*
University of Rochester, Rochester, New York 14627
(Received 8 July 1968)

A spectroscopic study of Sc^{44} up to an excitation energy of 5.5 MeV has been made using the Ca^{43} (He^3,d) Sc^{44} reaction. Observed angular distributions are compared with distorted-wave Born-approximation calculations, and spectroscopic strengths are extracted for transitions to pure as well as configuration-admixed states. Results are compared with theoretical calculations of the $(f_{7/2})^4$ spectrum. Most of the possible $f_{7/2}$ strength, but little of the possible $2p$ and $f_{5/2}$ strength, is observed.

INTRODUCTION

FEW odd-odd nuclei in the $1f_{7/2}$ shell have been investigated with single-particle stripping reactions. Thus, little is known about the extent of $1f$ and $2p$ shell mixing or the strength of the odd-pair coupling. Of the odd-odd nuclei which can be reached with a single-particle stripping reaction, Sc^{44} is most attractive for an initial study since its low-lying spectrum may be expected to be described with the smallest number of active particles and the lowest level density. In addition to numerous studies[1] of the two isomeric states in Sc^{44}, the nuclide has been studied only with the (d,α) (See Ref. 2) and (p,d) (See Ref. 3.) reactions up to excitation energies of 1.7 MeV. In the study reported here, the proton stripping on Ca^{43} is investigated with high resolution up to an excitation energy of 5.5 MeV in Sc^{44} in an attempt to obtain information on the amount of $1f$ and $2p$ shell mixing.

EXPERIMENTAL PROCEDURE

Measurements were carried out at the Physics Division of the Argonne National Laboratory using a 12-MeV He^3 beam from the tandem Van de Graaff accelerator. The target consisted of 50 μg/cm^2 of calcium enriched to 81% in Ca^{43} on a 165-μg/cm^2 gold backing. The target was prepared by reducing enriched $CaCO_3$ in a hot tantalum filament and evaporating the residual calcium onto the Au substrate. The target was withdrawn directly from the evacuated evaporator into a vacuum lock which was then attached to the scattering chamber. The target was all times at a pressure less than 10 μ Hg.

Emergent deuterons were detected in Kodak-type NTB emulsions placed in the focal plane of a 75-cm Brown-Buechner broad-range spectrograph. The emulsions were 100 μ thick with aluminum absorber sufficient to reduce the residual range of deuterons in the emulsion to about 100 μ in order to facilitate particle discrimination.

Angular distributions were taken over the range of 7.5° to 55° in 5° intervals. Exposures at different angles were normalized to the yield of the He^3 elastically scattered from the Ca^{43} and detected in a monitor counter at 90°. Absolute cross sections with an uncertainty of 25% were obtained by using a value of 0.13 for the ratio of the cross section of He^3 elastically scattered from Ca at 90° to the Rutherford cross section. This value was inferred from previous studies[4] of the Ca^{40}(He^3,He^3)Ca^{40} reaction.

RESULTS

Emergent deuteron groups corresponding to 83 energy levels of Sc^{44} were found. These energy levels are shown in Table I. A typical spectrum appears in Fig. 1. Distorted-wave Born-approximation (DWBA) calculations have been made for the angular distributions of the more prominent transitions. The calculations were made by Satchler at Oak Ridge National Laboratory using the code JULIE.[5] A Saxon-Woods potential was used for the bound-state potential which also contained a spin-orbit term. The depth of the bound-state potential well was adjusted to give the correct proton binding energy. A Saxon-Woods potential was also used for the optical potential, the parameters for which are the same as those used for previous analyses[6] of (He^3,d) reactions on calcium isotopes at this energy and are listed in Table II. No radial cutoff is used in these calculations since it has been found[6] to have little effect on the calculated cross sections at this energy. A zero-range interaction and local optical potential were used in all calculations. The measured and calculated cross sections are related by

$$\frac{d\sigma}{d\Omega}=\frac{2J_f+1}{2J_i+1}C^2S\times 4.4\left(\frac{d\sigma}{d\Omega}\right)_{\text{JULIE}}.$$

It has been found in other work[6] that the factor of 4.4 provides good agreement between measured and calculated cross sections for full-strength single-particle transitions. Examples of the angular distributions cal-

† Research supported by the U. S. Atomic Energy Commission.
* Present address: Stanford University, Stanford, Calif.
[1] J. K. Kliwer, J. J. Kraushaar, R. A. Ristinen, J. R. Keith, and A. A. Bartlett, Nucl. Phys. **49**, 328 (1963).
[2] J. H. Bjerregaard, P. F. Dahl, O. Hansen, and G. Sidenius, Nucl. Phys. **51**, 61 (1964).
[3] E. Kashy, Phys. Rev. **134**, B378 (1964).
[4] D. Cline, W. P. Alford, and L. M. Blau, Nucl. Phys. **73**, 33 (1965).
[5] G. R. Satchler, Nucl. Phys. **55**, 1 (1964).
[6] J. J. Schwartz and W. P. Alford, Phys. Rev. **149**, 820 (1966); J. J. Schwartz, W. P. Alford, and A. Marinov, *ibid.* **153**, 1248 (1967).

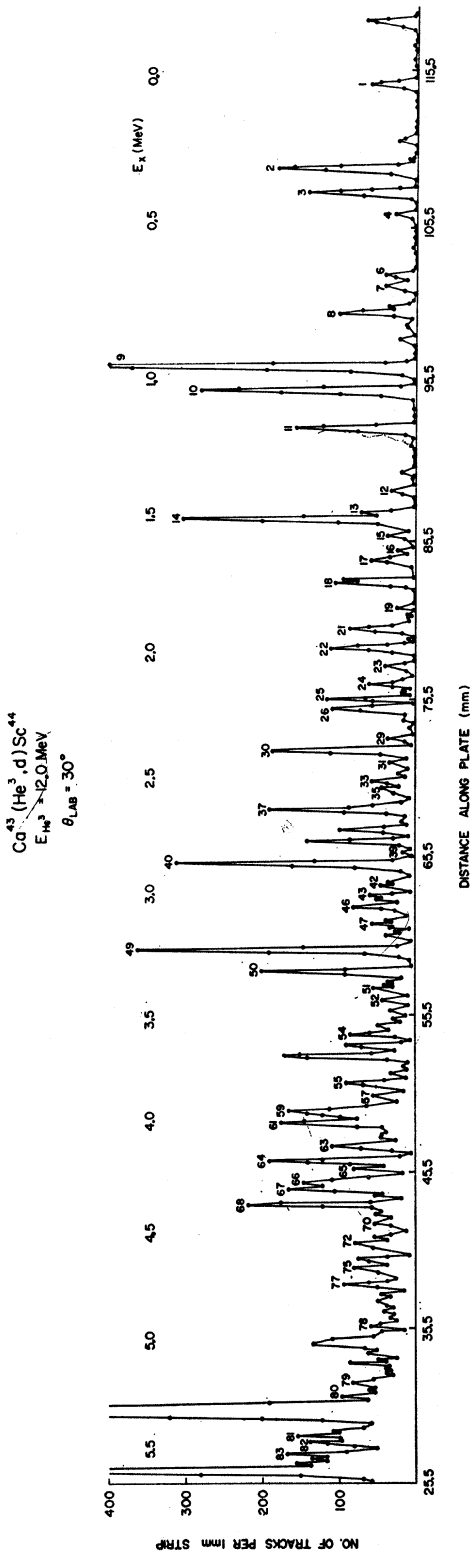

FIG. 1. Typical spectrum of emergent deuterons recorded in nuclear emulsions. Large unnumbered groups are due primarily to Ca^{44} contaminants in the target. Missing numbers indicate levels unobserved at this angle.

TABLE I. Energy levels and spectroscopic strengths in the $Ca^{43}(He^3,d)Sc^{44}$ reaction.

Level No.	E_x keV	$d\sigma/d\Omega$ peak mb/sr	l	$([J_f]/[J_i])C^2S(l)$
1	0	0.11	3	0.28
2	274±6	0.34	3	0.73
3	354±9	0.22	1, 3	0.023(1), 0.450(3)
4	429±13	0.04	1, 3	0.004(1), 0.084(3)
5	521±11	<0.05		
6	637±6	0.59	0	0.04
7	671±10	0.07	3	0.15
8	760±7	0.37	1, 3	0.055(1), 0.166(3)
9	980±10	0.76	3	1.62
10	1058±12	1.12	1, 3	0.170(1), 0.340(3)
11	1197±8	0.30	1, 3	0.024(1), 0.490(3)
12	1433±18	0.08	1, 3	0.010(1), 0.070(3)
13	1512±9	0.16	1, 3	0.020(1), 0.141(3)
14	1537±11	0.45	1, 3	0.038(1), 0.756(3)
15	1598±13	0.10	1, 3	0.014(1), 0.043(3)
16	1653±12	0.12	1	0.014
17	1683±9	0.12	2	0.17
18	1773±13	0.39	1, 3	0.049(1), 0.097(3)
19	1865±8	0.06	1	0.008
20	1903±11	<0.05		
21	1956±10	0.49	1	0.058
22	2035±10	0.33	1, 3	0.042(1), 0.084(3)
23	2104±6	0.13	1, 3	0.016(1), 0.032(3)
24	2173±11	0.15	1, 3	0.018(1), 0.055(3)
25	2250±14	0.13	3	0.19
26	2295±9	0.48	1, 3	0.062(1), 0.064(3)
27	2334±5	<0.05		
28	2383±5	<0.05		
29	2427±10	0.07	1, 3	0.007(1), 0.015(3)
30	2476±10	0.80	1, 3	0.010(1), 0.011(3)
31	2525±11	<0.05		
32	2556±10	<0.05		
33	2591±14	0.20	1, 3	0.024(1), 0.049(3)
34	2617±10	<0.05		
35	2632±11	0.05		
36	2684±10	<0.05		
37	2712±8	0.45	1, 3	0.058(1), 0.116(3)
38	2796±5	0.08	3	0.11
39	2878±9	<0.05		
40	2931±10	0.73	1, 3	0.076(1), 0.23(3)
41	3010±11	<0.05		
42	3035±10	0.05		
43	3049±10	0.08		
44	3071±8	0.13	1, 3	0.017(1), 0.067(3)
45	3097±10	0.25	1, 3	0.030(1), 0.031(3)
46	3152±10	0.15		
47	3176±8	0.08		
48	3204±7	<0.05		
49	3281±15	0.84	1, 3	0.093(1), 0.280(3)
50	3370±14	0.54	1, 3	0.060(1), 0.062(3)
51	3427±11	0.14	1	0.015
52	3483±12	0.14	1, 3	0.014(1), 0.029(3)
53	3568±6	<0.05		
54	3626±10	0.24	1, 3	0.026(1), 0.024(3)
55	3851±6	0.36	1	0.41
56	3967±12	<0.05		
57	4024±13	0.07		
58	4038±14	<0.05		
59	4053±15	0.19		
60	4087±7	0.48	1	0.055
61	4150±10	0.17		
62	4185±10	<0.05		
63	4254±11	0.27	1	0.034
64	4293±15	0.14	1, 3	0.015(1), 0.03(3)
65	4363±11	0.58	1	0.176
66	4391±14	0.16	3	0.186
67	4461±14	0.42	1, 3	0.048(1), 0.045(3)
68	4500±16	0.25		
69	4533±10	0.20	1	0.024
70	4595±10	<0.05		
71	4622±12	<0.05		
72	4645±14	0.07		

TABLE I. (*continued*).

Level No.	E_x keV	$d\sigma/d\Omega$ peak mb/sr	l	$([J_f]/[J_i])C^2S(l)$
73	4697±10	0.17	1, 3	0.022(1), 0.023(3)
74	4746±14	0.08	2	0.68
75	4762±10	0.08		
76	4820±10	0.21	1	0.025
77	5012±15	0.10		
78	5277±10	<0.05		
79	5336±6	<0.05		
80	5526±13	0.13	3	0.15
81	5553±11	0.11	2	0.14
82	5608±5	<0.05		
83	5716±13	<0.05		

culated for various orbital angular momentum transfers are shown in Fig. 2.

The significant difference in the shape of the angular distributions of transitions with different orbital angular momentum transfer facilitates the determination of the relative contribution of s, p, d, and f waves to each transition. As a result, admixtures as small as 13% in the cross section for a transition are readily observed. In particular, numerous states of Sc^{44} appear to be reached with f waves, p waves, or a mixture of both. In these cases, a least-squares fit of a linear combination of p and f waves to the data was made in order to extract the $l=1$ and $l=3$ contributions to the transition. It is found that a number of states are reached with either p or f waves comprising at least 87% of the transition cross section. These transitions are referred to here as being "pure" and their angular distributions are shown in Figs. 3 and 4.

The Sc^{44} analog to the Ca^{44} ground state is known[7] to lie at 2.796 MeV. However, this level was not resolved from the known 2.979-MeV level of Sc^{45} which is present due to a small Ca^{44} contamination in the target. It is known[8] that the latter level is reached with a p wave and the 2.796-MeV level of Sc^{44} is necessarily reached with an f wave. Thus, as shown in the upper curve of Fig. 5, the angular distribution of the emergent deuterons at an energy corresponding to this 0+ analog state is fit quite well with a mixture of $l=1$ and $l=3$. When the

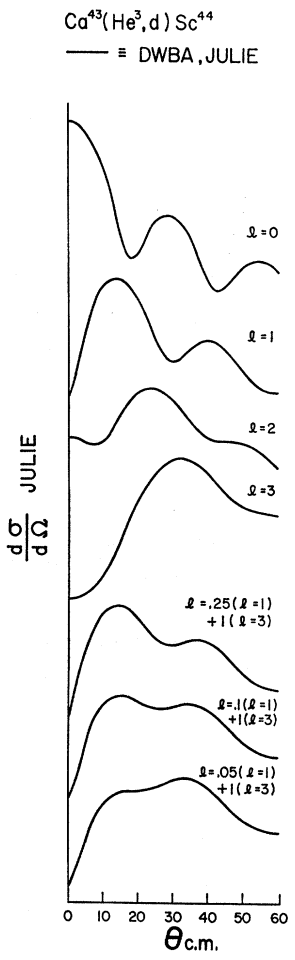

FIG. 2. DWBA calculations of the angular distributions for the $Ca^{43}(He^3,d)Sc^{44}$ reactions for various orbital angular momentum transfers.

TABLE II. Optical-model expressions and parameters used in analysis of $Ca^{43}(He^3,d)Sc^{44}$ data. Well depths are given in MeV and lengths in fermis.

$$U(r)=-V(e^x+1)^{-1}-i[W-4W_d(d/dx')](e^{x'}+1)^{-1}+U_c(r),$$

where

$$U_c(r)=(Ze^2/2R_c)(3-r^2/R_c^2), \quad r<R_c$$
$$=Ze^2/r, \quad r\geq R_c$$
$$x'=(r-r_0'A^{1/3})/\alpha', \quad x=(r-r_0A^{1/3})/\alpha,$$
$$R_c=r_cA^{1/3}.$$

Spin-orbit potential:

$$U_{so}(r)=(\hbar/m_\pi c)^2(V_s+iW_s)(1/r)(d/dr)(e^x+1)^{-1}\mathbf{L}\cdot\mathbf{S}.$$

	V	W	r_0	r_c	α	V_s	W_s	r_0'	α'	W_d
Entrance channel	168.0	17.0	1.07	1.4	0.854	0	0	1.81	0.592	0
Exit channel	112.0	0	1.0	1.3	0.900	0	0	1.55	0.470	18.0
Bound state			1.2	1.25	0.65	8.0				

[7] J. A. Nolen, Jr., J. P. Schiffer, N. Williams, and D. von Ehrenstein, Phys. Rev. Letters **18**, 1140 (1967).
[8] J. J. Schwartz and W. P. Alford, Phys. Rev. **149**, 820 (1966).

TABLE III. Data on states reached primarily by f-wave transitions compared with theoretical $(f_{7/2})^4$ calculations.

Experiment				Theory $(f_{7/2})^4$ [a]		
E_x (MeV)	Relative p, f wave components	$[J_f/J_i]\, C^2S_f$	$J; T$	E_x (MeV)	$[J_f/J_i]\, C^2S$	$J; T$
0.0	pure f	0.28	2; 1	0.0	0.33	2; 1
0.274	pure f	0.73	6; 1	0.36	0.73	6; 1
0.354	0.048 p+1f	0.45	(3,4); 1	0.44	0.10	1; 1
0.671	pure f	0.15	1; 1	0.66	0.68	4; 1
0.980	pure f	1.62	7; 1	0.75	0.43	3; 1
1.197	0.044 p+1f	0.48	(3,4); 1	1.22	1.66	7; 1
1.537	0.053 p+1f	0.75	5; 1	1.23	1.12	5; 1
2.250	pure f	0.19	(1,6); 1	2.16	0.18	3; 1
2.796	pure f	0.11	0; 2	2.18	0.27	6; 1
4.391	pure f	0.19		2.30	0.28	1; 1
5.526	pure f	0.15		2.53	0.08	2; 1
				2.95	0.12	0; 2
				3.04	0.25	3; 1
				3.27	0.19	7; 1
				4.00	0.10	5; 1
				4.53	0.21	2; 2
				5.70	0.38	4; 2
				6.14	0.54	6; 2

[a] States with $[J_f/J_i]C^2S$ less than 0.05 have been excluded from the table. Thus, slightly less than the total possible strength is accounted for with the levels tabulated here.

p-wave contribution is subtracted out, the remaining angular distribution (shown in the lower curve on Fig. 5) represents that of transitions to the 2.796-MeV level

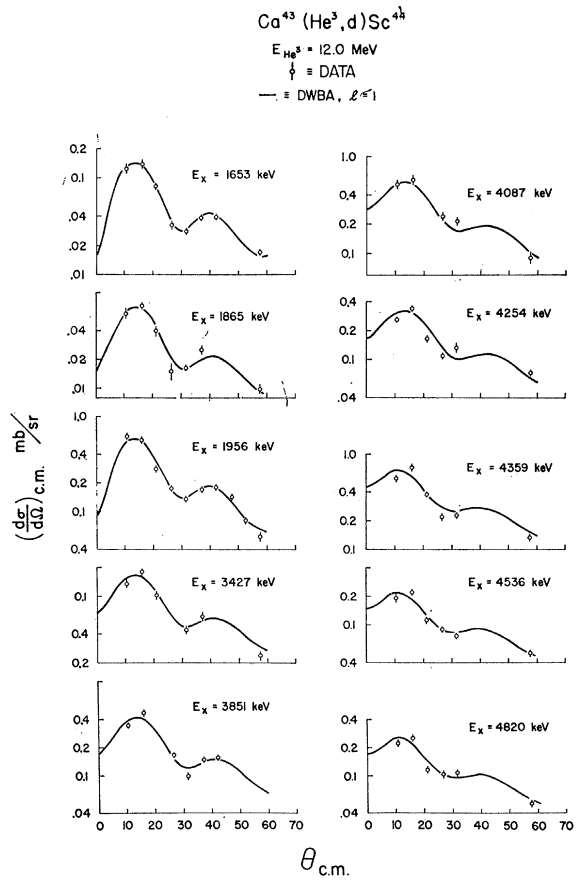

FIG. 3. Angular distributions of p-wave transitions (with f-wave admixtures less than 13% in cross section).

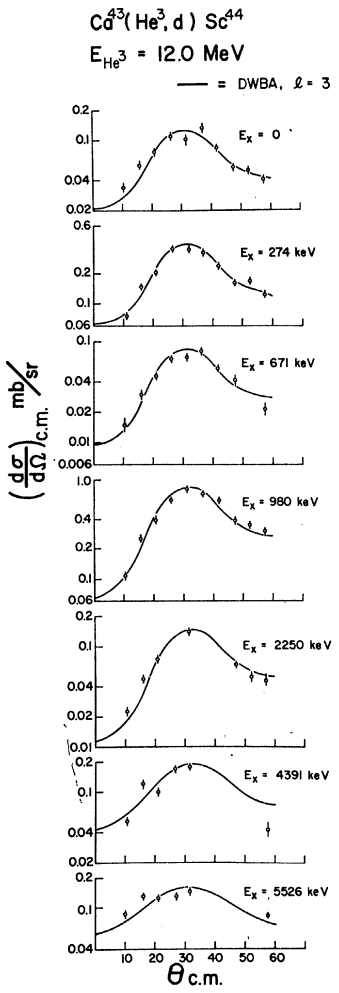

FIG. 4. Angular distributions of f-wave transitions (with p-wave admixtures less than 13% in cross section).

of Sc^{44}. Numerous other states are seen to be reached with a significant mixture of f and p waves and the angular distributions of these transitions together with the amount of f and p strength in each mixture are shown in Fig. 6. The distributions of f and p-wave strength are shown in Fig. 7.

It is of interest to compare the observed distribution of f wave strength with that expected from a pure $(f_{7/2})^4$ configuration. The Rochester–Oak-Ridge shell-model program[9] was used to calculate the expected level structure of the Sc^{44} $(f_{7/2})^4$ configuration as well as the expected distribution of $f_{7/2}$ spectroscopic strength for this reaction. The two-body spectrum used for the effective interaction in these computations was taken from recent studies[10] of the Sc^{42} spectrum. Agreement with these calculations will depend, of course, on the goodness of the effective interaction used and the amount of core excitation in the Ca^{43} target nucleus. The results of this calculation are shown in Table III, together with the corresponding experimental results. The Sc^{44} levels observed at 0.0, 0.274, and 2.796 MeV are known[1,7,11] to have spins 2^+, 6^+, and 0^+, respectively; while a spin of 7^+ has been suggested[3] for the 0.980-MeV state. As shown in Fig. 2, there is no p-wave admixture in the 2^+ ground state and no such admixtures are possible in the 6^+, 0^+, and 7^+ levels. The 6^+ and 2^+ levels are not likely to contain $f_{5/2}$ admixtures due to their low excitation energy. It is apparent from Table III that the theoretical excitation energies and spectroscopic strengths for these states agree extremely well with the experimental results. It is, therefore, suggested that the 1^+ state which, similarily, should contain no $p_{3/2}$ and only little $f_{5/2}$ admixture is probably also well described by the theoretical calculations. If so, the only reasonable choice for the 1^+ state is the 0.671-MeV level. The calculations further indicate that the 5^+ state is most likely either the 1.197 or 1.527-MeV level. The observed spectroscopic strength would favor the 1.537-MeV state. With a spin of 5^+ assigned to the 1.537-MeV level, the 0.354 and 1.197-MeV states would appear to have $J^\pi = 3^+$ or 4^+. The Sc^{44} analogs to the 2^+ and 4^+ states of Ca^{44} should lie at 3.95 and 5.07 MeV, respectively; but these states could not be unambiguously identified in this study.

It appears that below 1.6 MeV the configuration mixing with the $2p$ shell is rather small. The ground state shows no p-shell admixture while the states with spins 3^+, 4^+, or 5^+ show only small admixtures. In this region of excitation energy, the only state appearing highly

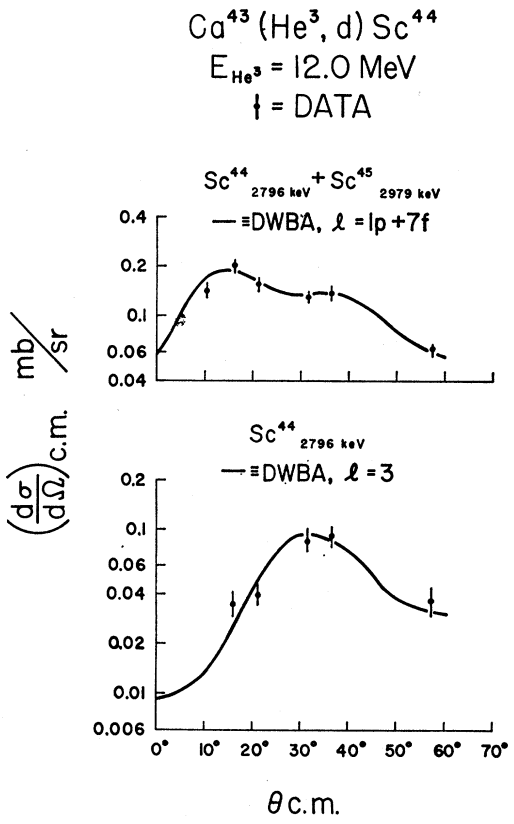

FIG. 5. Angular distributions of deuterons leading to the 2.796- and 2.979-MeV states of Sc^{44} and Sc^{45}, respectively (upper curve); with p-wave portion of this angular distribution subtracted (lower curve).

admixed with the $2p$ shell is the 1.058-MeV level. In contrast, the transitions to levels above 1.6 MeV in excitation are, in general, rather weak with considerably greater admixtures of p and f wave. From Table 1, it is seen that the total f-wave strength observed up to 5.5 MeV is about 7, i.e., $([J_f]/[J_i])C^2S = 7$ holes in the $f_{5/2}+f_{7/2}$ shells. It should be noted that about five holes are accounted for in the first 1.6 MeV of excitation where the $f_{5/2}$ contribution should be quite small. It is, therefore, suggested that most of the observed f-wave strength corresponds to $f_{7/2}$ transitions and little $f_{5/2}$ strength is found below 5.5 MeV. It is surprising that the total p-wave strength observed below this excitation energy is only two out of a possible six. However, the p-wave strength appears to be highly mixed and fragmented into many weak transitions and in such cases the spectroscopic strength extracted via the usual DWBA calculations may be quite unreliable.

Transitions to negative-parity states are also observed and their angular distributions appear in Fig. 8. The spectroscopic strength $\sum([J_f]/[J_i])C^2S$ is found to be 0.04 and 1.0 for the s- and d-wave transitions, respec-

[9] S. S. M. Wong, thesis, University of Rochester, 1966 (unpublished).
[10] J. J. Schwartz, D. Cline, H. E. Gove, R. Sherr, T. S. Bhatia, and R. H. Siemssen, Phys. Rev. Letters **19**, 1482 (1967).
[11] L. G. Mann, S. D. Bloom, and R. J. Nagle, Nucl. Phys. **30**, 636 (1962).

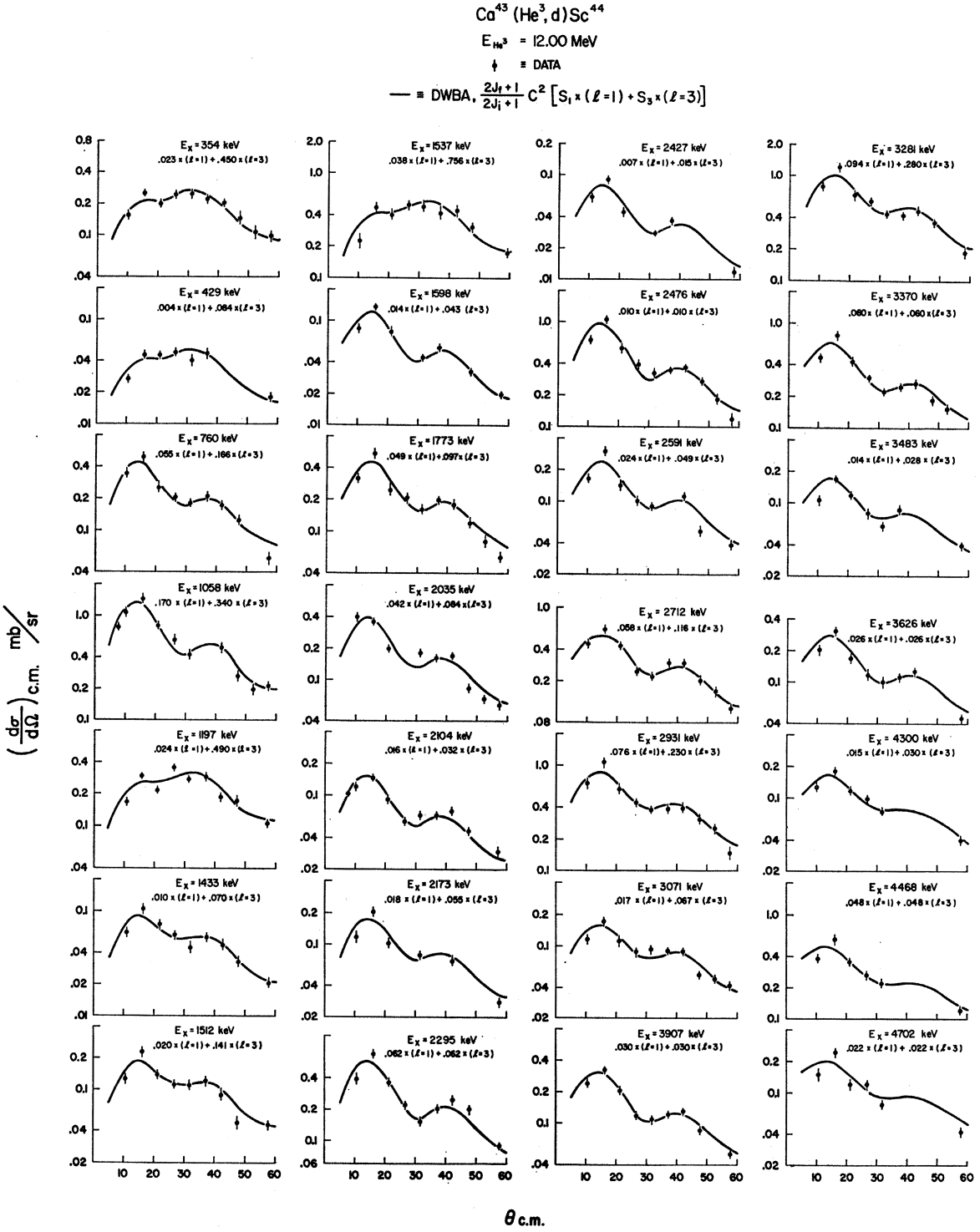

FIG. 6. Angular distributions of p- and f-wave admixed transitions.

tively. This is in good agreement with the d-wave strength observed in $Ca^{42,44}(He^3,d)Sc^{43,45}$ studies.[8] However, the s-wave strength observed here is an order of magnitude less than that observed in those studies. It is surprising that the 0.637-MeV level reached with an s wave lies 1 MeV lower than the lowest states reached

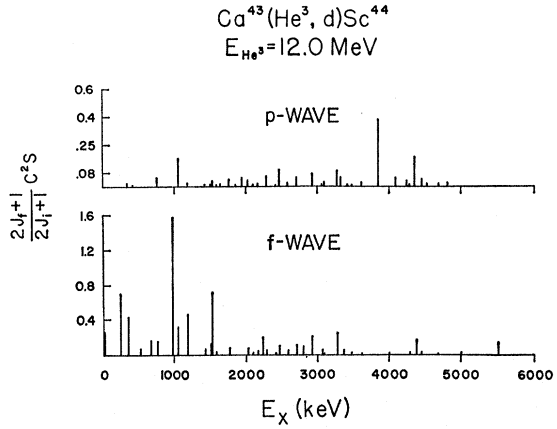

FIG. 7. Distribution of f- and p-wave spectroscopic strength.

with a d wave. This is not the case in Sc^{43}, Sc^{45}, or Sc^{47} where, as expected, the first d-hole state lies at least 0.5 MeV below the lowest s state.[6] It is also of interest to note that the state at 1.683 MeV reached with a d-wave in this reaction also appears to be reached with a d-wave in the Sc^{45} (p,d) Sc^{44} reaction,[3] indicating that this state must be described by both proton and neutron holes in the 2d shell.

SUMMARY

The observed angular distributions of emergent deuterons are fit quite well with DWBA calculations and are, therefore, characteristic of a single-particle stripping reaction. Those Sc^{44} states such as the 0^+, 1^+, 2^+, 6^+, and 7^+ levels which appear to be reached with pure $f_{7/2}$ transitions are described extremely well by theoretical calculations of the $(f_{7/2})^4$ energy spectrum and transition strength. Below 1.6 MeV in excitation, the $1f$ and $2p$ mixing appears to be fairly small. Above 1.6 MeV in excitation the observed transitions are, in general, quite weak and well mixed with f and p waves. Most of the f-wave strength leading to levels below 5.5 MeV in excitation is attributed to $f_{7/2}$ transitions. Relatively little p-wave strength is observed and this small amount of strength appears highly mixed and fragmented among many weak transitions.

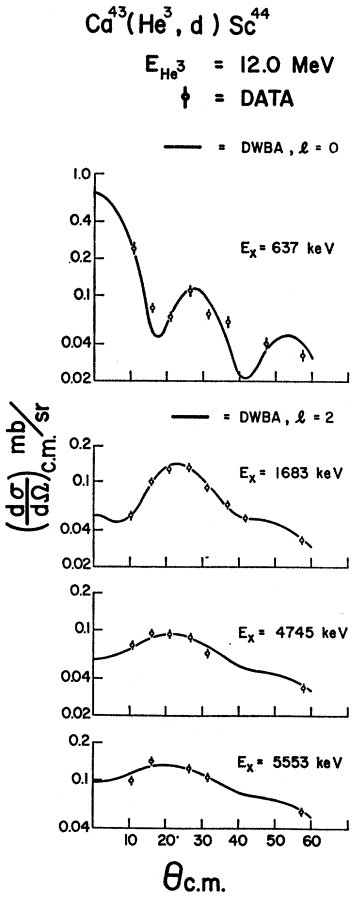

FIG. 8. Angular distribution of s- and d-wave transitions.

ACKNOWLEDGMENTS

The author is grateful to the Physics Division of the Argonne National Laboratory for the use of the tandem Van de Graaff accelerator and to the National Science Foundation for its support during the subsequent analysis of the data. The author is also indebted to G. R. Satchler for making the DWBA calculations, A. Jamshidi for his aid in analyzing the data, and Professor W. P. Alford and Dr. M. Moinester for numerous helpful discussions.